In-plane sixfold symmetry for α-Fe(110) on GaN{0001}: Measurement of the cubic anisotropy constant K_3 of Fe

Cunxu Gao,* Chunhui Dong, Chenglong Jia, and Desheng Xue†
Key Lab for Magnetism and Magnetic Materials of the Ministry of Education, Lanzhou University, 730000 Lanzhou, P. R. China

Jens Herfort and Oliver Brandt
Paul-Drude-Institut für Festkörperelektronik, Hausvogteiplatz 5–7, 10117 Berlin, Germany
(Received 8 July 2015; revised manuscript received 11 August 2015; published 1 September 2015)

We investigate the magnetic anisotropy of epitaxial Fe films on GaN(0001) and GaN(000$\bar{1}$). Due to the particular orientation relationship between Fe and GaN{0001}, the leading term proportional to K_1 does not contribute to the magnetic anisotropy, allowing us to determine K_3 with unprecedented accuracy. Using two experimental techniques, we obtain values for K_3 of 4.7–9.2 $\times$ 10^5 erg/cm^3, i.e., comparable to and even larger than K_1.

DOI: 10.1103/PhysRevB.92.094404 PACS number(s): 75.30.Gw, 61.50.Ah, 75.50.Bb, 81.15.Hi

The magnetocrystalline anisotropy of a ferromagnet is determined by its crystal structure and is thus an inherent source of magnetic anisotropy [1,2]. It is the key to an understanding of ferromagnetism itself and has been the subject of innumerable studies but is still a problem far from being solved completely [3]. Consequently, magnetocrystalline anisotropy is still actively investigated [4,5] even for apparently well-understood materials such as Fe [6–8].

For cubic crystals such as Fe, the magnetocrystalline anisotropy energy can be expressed in terms of the direction cosines α_1, α_2, and α_3 of the magnetization vector with respect to the three cube edges. Considering the total magnetic anisotropy energy ϵ to be composed of the magnetocrystalline energy ϵ_A, the Zeeman energy ϵ_H, and the demagnetizing energy ϵ_D, we can write up to third order

$$\begin{aligned}\epsilon &= \epsilon_A + \epsilon_H + \epsilon_D \\ &= K_1\left(\alpha_1^2\alpha_2^2 + \alpha_2^2\alpha_3^2 + \alpha_3^2\alpha_1^2\right) + K_2\alpha_1^2\alpha_2^2\alpha_3^2 \\ &\quad + K_3\left(\alpha_1^2\alpha_2^2 + \alpha_2^2\alpha_3^2 + \alpha_3^2\alpha_1^2\right)^2 \\ &\quad - HM_s\sin\theta\cos(\phi-\phi_0) + 2\pi M_s^2\cos^2\theta, \qquad (1)\end{aligned}$$

where K_1, K_2, and K_3 are the cubic anisotropy constants [9], θ is the polar angle between the saturation magnetization M_S and the out-of-plane direction, and ϕ is the azimuthal angle between the projection of M_S and the in-plane easy axis. ϕ_0 is the in-plane azimuthal angle between the direction of the external magnetic field H and the easy axis. The various angles are shown in the schematic coordinate system depicted in Fig. 1(a). Equation (1) neglects terms related to uniaxial terms mainly originating from interface and/or surface effects. For thin films such as investigated in the present work, the magnetization is considered to lie in-plane, i.e., $\theta = \pi/2$.

Values for any of the anisotropy constants have been derived exclusively from experiments. In fact, the magnetocrystalline anisotropy has turned out to be virtually inaccessible to first-principles calculations. The main reason for this fact is the magnitude of the magnetocrystalline anisotropy energy of only a few micro–electron volts per atom, the resolution of which requires an accuracy unattainable even with today's computational resources [3]. Experimentally, however, it is rather straightforward to determine the leading term of the expansion shown in Eq. (1), and reliable values of about 4.7×10^5 erg/cm^3 for K_1 of Fe have been measured already in early studies [10,11].

The determination of the higher-order anisotropy constants K_2 and K_3 is far more difficult, since their prefactors are of sixth and eighth order, respectively, and decrease correspondingly in magnitude. The fourth-order term proportional to K_1 is thus expected to dominate the magnetic anisotropy regardless of the magnitude of K_2 and K_3, and the accuracy of the measurement is insufficient to detect the small deviations introduced by the higher-order terms [12]. Due to this difficulty, and the belief that the higher-order anisotropy constants will be smaller than K_1 in any case, it is frequently assumed that a single anisotropy constant suffices to describe the anisotropy energy with a good accuracy [13].

The difficulty of experimentally determining the higher-order anisotropy constants is illustrated in Table I for the major low-index orientations of Fe. For single-crystal Fe(001), for example, the magnetocrystalline anisotropy arises from the terms proportional to K_1 and K_3 (denoted "$\times$"), while the term proportional to K_2 does not depend on the azimuthal angle ϕ. In other words, it is isotropic (represented by "$\circ$") and will thus not contribute to the magnetic anisotropy. Obviously, Fe films with this orientation will not be suitable for measuring K_3 because the anisotropy will be governed by the leading term proportional to K_1. The sensitivity for these higher-order constants is even worse for single-crystal Fe(101) films, for which all terms contribute to the magnetic anisotropy.

For single-crystal Fe(111), however, we encounter a radically different situation. In this case, the only anisotropic term is the one proportional to K_2, and careful experiments (allowing for the presence of a uniaxial anisotropy due to interface effects) should be able to directly measure the value of K_2. In fact, several groups have recognized this opportunity and performed experiments aimed for a determination of K_2 on Fe(111) films [14,15]. Early experiments on bulk Fe

*gaocunx@lzu.edu.cn
†xueds@lzu.edu.cn

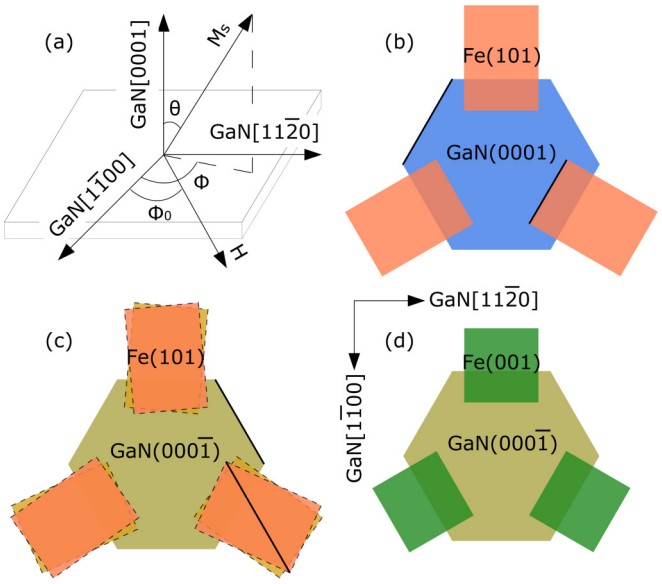

FIG. 1. (Color online) (a) Schematic coordinate system showing the various angles appearing in Eq. (1). θ is the polar angle of M_S with respect to the out-of-plane axis (i.e., GaN[0001]). The external field (H) is applied parallel to the sample surface. ϕ_0 is the azimuthal angle between the direction of H and the in-plane easy axis (i.e., GaN[1$\bar{1}$00]). ϕ is the azimuthal angle between the projection of M_S on the sample surface and the in-plane easy axis. (b–d) Schematic of the (b) Pitsch-Schrader, (c) Burgers, and (d) cube-on-hexagon orientation relationships of Fe (rectangle or square) on GaN{0001} (hexagon). The difference in lattice constants has been exaggerated for clarity. The solid lines in (b) and (c) show the angular relation of the unit cells. The dashed lines in (c) enhance the visibility of the domains rotated by ±5.26°.

were hampered by the dominance of K_1, and one could only state with certainty that K_2 is in the range of $(0 \pm 5) \times 10^4$ erg/cm^3. Recently, researchers using the unique configuration encountered for Fe(111) films have been able to improve the accuracy by orders of magnitude, resulting in a value of $K_2 = (2.2 \pm 0.1) \times 10^4$ erg/cm^3 [6,7].

There is no analogous situation for the determination of K_3; i.e., no crystal orientation exists for which this term would be the only one being anisotropic. In the present work, we use epitaxial Fe films on GaN{0001}, which exhibit crystallographic orientation relationships for which the K_1 term does not contribute to the magnetocrystalline anisotropy (cf. Table I). In fact, the K_1 term cancels due to the superposition of the multiple domains of the respective orientation relationship. In other words, only the K_2 and K_3 terms exhibit an azimuthal angular dependence, and the magnetic anisotropy measured is thus solely due to these higher-order terms. This materials system thus offers the unique opportunity to determine the value of K_3 of Fe with a high accuracy.

The structures investigated were grown in a custom-built molecular beam epitaxy system equipped with solid-source effusion cells for Ga and Fe. Active nitrogen was provided by a radiofrequency N_2 plasma source. Nucleation and growth were monitored *in situ* by reflection high-energy electron diffraction (RHEED). A 300-nm GaN layer was grown by molecular beam epitaxy on GaN(0001) templates and on Al_2O_3(0001)

TABLE I. Azimuthal dependence of the first three terms of ϵ_A as given by Eq. (1) for the major low-index orientations of Fe and the multiple-domain orientation relationships obtained in the epitaxial growth of Fe on GaN{0001}. If the term depends on ϕ, it is denoted "×"; otherwise, "○."

Orientation	K_1	K_2	K_3
(001)	×	○	×
(101)	×	×	×
(111)	○	×	○
Cube-on-hexagon	○	○	○
Pitsch-Schrader	○	×	×
Burgers	○	×	×

substrates to obtain Ga- and N-polar GaN surfaces, respectively. Directly after growth of the GaN layer, excess Ga was desorbed prior to cooling down to 500°C (350°C) for the Ga-polar (N-polar) GaN surface on which Fe deposition was initiated. Fe growth then occurred at the selected temperature at a rate of 0.12 nm/min, keeping the chamber pressure in the low 10^{-9} mb range until a final thickness of 30 nm was reached. Electron backscatter diffraction was employed *ex situ* to obtain the crystal structure and orientational distribution of the Fe film in a direct and unambiguous way. Electron backscatter diffraction maps visualize the domain structure of the Fe film on a nanometer spatial scale with an angular resolution of better than 1° [16]. The orientation relationship between Fe and GaN was assessed by high-resolution x-ray diffractometry (HRXRD) [16]. HRXRD longitudinal Θ-2Θ scans were recorded with a Ge analyzer crystal with a dynamic range of at least five orders of magnitude, showing no reflections pertinent to a secondary phase, while azimuthal Φ scans were taken with an open detector. The in-plane orientation distribution was measured with an angular resolution of 0.01°. The out-of-plane magnetization was measured at 300 K for magnetic fields between ±50 kOe in a superconducting quantum interference device magnetometer (SQUID). In-plane hysteresis loops were recorded at room temperature for magnetic fields between ±20 kOe by vibrating sample magnetometry (VSM). All data presented in hysteresis loops were corrected for the diamagnetic background of the substrate. The in-plane magnetic anisotropy of the films was assessed by both rotational magnetization curves (RMCs) obtained from the angular dependence of magnetization measured by VSM and ferromagnetic resonance (FMR).

The lattice mismatch between Fe and GaN(0001) is −10% and −27% along the GaN[11$\bar{2}$0] and GaN[1$\bar{1}$00] directions, respectively. As a consequence, strain relaxation occurs instantaneously and is completed within the first monolayers of Fe deposition. This fact is evidenced experimentally by RHEED and theoretically supported by density-functional theory calculations (see Ref. [16]). Consequently, thick (tens of nanometers) films do not exhibit any net strain as evidenced by HRXRD (see Ref. [16]) and exhibit bulk-like properties. The orientation relationships of α-Fe films on GaN{0001} were systematically studied in our previous work [16–19] and are schematically summarized in Fig. 1. Fe on GaN(0001) [Fig. 1(a)] exhibits a pure Pitsch-Schrader orientation relationship formed by three symmetry-equivalent domains

with Fe(101)⟨010⟩‖GaN(0001)⟨11$\bar{2}$0⟩ rotated by 120° relative to each other. In contrast, for Fe on GaN(000$\bar{1}$), a coexistence of the Burgers [Fig. 1(b)] and "cube-on-hexagon" [Fig. 1(c)] orientation relationships is observed. The former consists of six symmetry-equivalent domains each produced from a single Pitsch-Schrader domain by a ±5.26° rotation around the Fe[101] axis (which is the angle between the ⟨010⟩ and the ⟨11$\bar{1}$⟩ and ⟨1$\bar{1}\bar{1}$⟩ axes), the latter of three symmetry-equivalent domains with Fe(001)⟨010⟩‖GaN(0001)⟨11$\bar{2}$0⟩ rotated by 120° relative to each other. Each of the symmetry-equivalent domains for all of these orientation relationships manifests itself by a distinct reflection in HRXRD azimuthal Φ scans. The equal intensity of these reflections directly shows that these symmetry-equivalent domains have identical area fractions on a macroscopic scale.

Figure 2 shows normalized in-plane hysteresis loops for Fe films grown on GaN(0001) [Fig. 2(a)] and GaN(000$\bar{1}$) [Fig. 2(b)] surfaces measured by VSM with the magnetic field parallel and perpendicular to the GaN[1$\bar{1}$00] direction at room temperature. The saturation magnetization M_S is found to be 1340 and 1390 emu/cm^3 for Fe films on GaN(0001) and GaN(000$\bar{1}$), respectively. These values are consistent with the average value of 1350 emu/cm^3 obtained in Ref. [17] and are lower than the saturation magnetization of bulk Fe only because the contribution of the FeO_x layer to the total thickness of the film was not taken into account [19]. For either of these samples, the hysteresis loops taken along orthogonal directions are virtually identical, indicating a very small in-plane magnetic anisotropy. This finding is confirmed by the azimuthal dependence of the coercivities as shown in Fig. 2(c). The nearly isotropic behavior originates from the superposition of the multiple domains of the respective orientation relationships. Out-of-plane measurements by SQUID (not shown here) reveal a pure hard axis for both samples, with no sign of an admixture of the in-plane easy axes. It is thus justified to assume an infinitely strong demagnetization field of $4\pi M_S$ which forces the magnetization to lie strictly in the film plane.

To investigate the magnetic anisotropy of these films with a higher sensitivity, the Fe films were investigated by in-plane RMC obtained by VSM. For these RMC experiments, Fe films on GaN(0001) [GaN(000$\bar{1}$)] were first magnetized in-plane at a field of 20 kOe for 5 s, followed by a decrease in the field to 200 Oe (100 Oe) to discard the irreversible part of the magnetization loop. We then measured the projection of M_S in the field direction with the sample slowly rotated around its out-of-plane axis (i. e., GaN[0001]) [20,21]. Figure 3 shows the resulting RMCs as a function of ϕ_0. Both samples are seen to exhibit a clear sixfold in-plane anisotropy, with the in-plane easy and hard axes along the GaN⟨1$\bar{1}$00⟩ and GaN⟨11$\bar{2}$0⟩ directions, respectively.

For a quantitative understanding of this result, we determine the magnetocrystalline anisotropy expected for our samples with the help of Eq. (1). We start from a single Pitsch-Schrader domain with Fe(101)⟨010⟩‖GaN(0001)⟨11$\bar{2}$0⟩ and obtain, in agreement with Ref. [9],

$$\epsilon_A = \tfrac{1}{32}K_1(7+4\cos 2\phi-3\cos 4\phi)+\tfrac{1}{128}K_2(2+2\cos 2\phi - 2\cos 4\phi-\cos 6\phi)+\tfrac{1}{2048}K_3(123+88\cos 2\phi - 68\cos 4\phi-24\cos 6\phi+9\cos 8\phi). \quad (2)$$

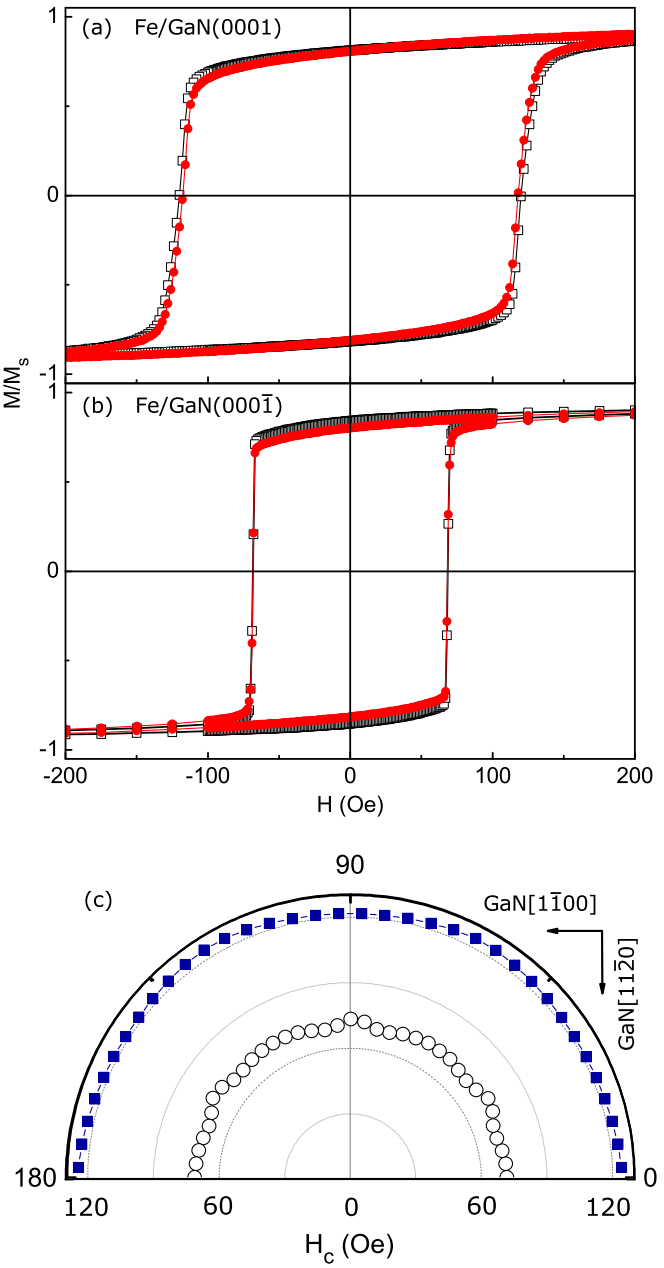

FIG. 2. (Color online) In-plane magnetic hysteresis loops of Fe films on (a) GaN(0001) and (b) GaN(000$\bar{1}$) obtained at room temperature with the magnetic field (H) parallel (open black squares) and perpendicular [filled (red) circles] to the GaN[1$\bar{1}$00] direction. (c) Semipolar plot of in-plane azimuthal dependence of coercivities H_c for Fe films on GaN(0001) [filled (blue) squares] and GaN(000$\bar{1}$) (open black circles).

In our Fe/GaN(0001) samples, we have three Pitsch-Schrader domains. The general expression of the total anisotropy energy is an area-weighted mean of the three domains, which is used afterwards for the analyis of the experimental results. The corresponding expressions, however, are too bulky to be reproduced here and do not aid the understanding of the sixfold symmetry shown in Fig. 3. This understanding can be gained by assuming that the area fraction of each domain is precisely 1/3, for which we have to calculate simply $[\epsilon_A(\phi)+\epsilon_A(\phi+$

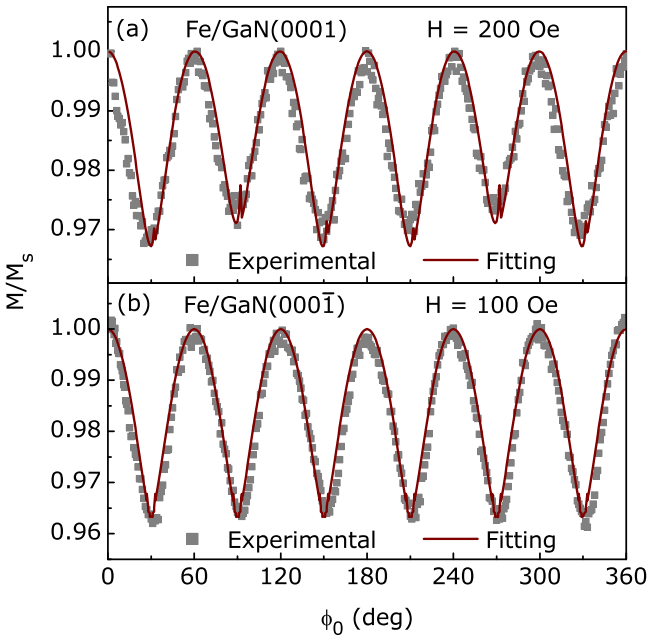

FIG. 3. (Color online) In-plane normalized RMCs of Fe films on (a) GaN(0001) and (b) GaN(000$\bar{1}$) obtained at room temperature with the magnetic field (H) parallel to the films' surfaces. Solid lines are fits as explained in the text.

$120^\circ) + \epsilon_A(\phi + 240^\circ)]/3$. The average anisotropy energy is then given by

$$\epsilon_A^{0001} = \epsilon_A^{\mathrm{PS}} = \tfrac{7}{32}K_1 + \tfrac{1}{64}K_2 + \tfrac{123}{2048}K_3 - \tfrac{1}{256}(2K_2 + 3K_3)\cos 6\phi, \quad (3)$$

in which the K_1 term does not depend on the azimuthal angle ϕ. In addition, the only remaining dependence on ϕ results in a sixfold symmetry.

We proceed in the same way for Fe/GaN(000$\bar{1}$). The average anisotropy energy of the three cube-on-hexagon domains $\epsilon_A^{\mathrm{CoH}} = \frac{1}{8}K_1 + \frac{3}{128}K_3$ is independent of the in-plane azimuthal angle. The six Burgers domains can be considered to consist of two sets of PS domains rotated in-plane by $\pm 5.26^\circ$, resulting in anisotropy energies $\epsilon_A^{\mathrm{PS}}(\phi + 5.26^\circ)$ and $\epsilon_A^{\mathrm{PS}}(\phi - 5.26^\circ)$. Thus, the anisotropy energy, averaged over the six Burgers and the three cube-on-hexagon domains, is given by

$$\epsilon_A^{000\bar{1}} = \tfrac{3}{16}K_1 + \tfrac{1}{96}K_2 + \tfrac{49}{1024}K_3 - \tfrac{1}{384}\cos(31.56^\circ)(2K_2 + 3K_3)\cos 6\phi. \quad (4)$$

As for the case of Fe/GaN(0001), the K_1 term does not depend on ϕ. In other words, the only contributions to the in-plane magnetic anisotropy of Fe layers on both GaN(0001) and GaN(000$\bar{1}$) stem from K_2 and K_3. Note that this statement also applies to the uniaxial anisotropy originating from an anisotropic interface between Fe and GaN(0001) [8], which drops out as well when averaging over the multiple domains.

For a fit of the in-plane RMC, we assume that the magnetization reversal proceeds by coherent rotation. The equilibrium direction of magnetization is determined by the local minimum of the magnetic free energy ϵ, which is obtained by setting $\partial\epsilon/\partial\phi = 0$ and $\partial^2\epsilon/\partial\phi^2 > 0$:

$$\sin(6\phi) - \frac{H}{6A_3/M_s}\sin(\phi - \phi_0) = 0, \quad (5)$$

$$\cos(6\phi) - \frac{H}{36A_3/M_s}\cos(\phi - \phi_0) > 0, \quad (6)$$

with the effective anisotropy constant $A_3 = -\frac{1}{256}(2K_2 + 3K_3)$ for Fe films on GaN(0001) and $A_3 = -\frac{1}{384}\cos(31.56^\circ)(2K_2 + 3K_3)$ for Fe films on GaN(000$\bar{1}$). Fitting the experimental data with the simplified expressions deduced with the assumption of an exactly equal area fraction yields a value of A_3 equal to -1.06×10^4 and -6.23×10^3 erg/cm^3 for Fe films on GaN(0001) and GaN(000$\bar{1}$), respectively.

The experimental data, particular those for the Fe film on GaN(0001) [Fig. 3(a)], do not exhibit a perfect sinusodial shape but are modulated with an amplitude depending on ϕ_0. To account for this observation, we allow the area fractions to be distributed unequally and thus do not use Eqs. (5) and (6), but the analogous full expression derived from Eq. (2) and a corresponding one for Fe on GaN(000$\bar{1}$). For the data shown in Fig. 3(a), the best fit was obtained for area fractions of 0.339, 0.331, and 0.330, a very slight deviation from an equal distribution and consistent with our HRXRD results within the error bar of these experiments. The best fit for the data shown in Fig. 3(b) returned equal area fractions of 0.333. The values of A_3 obtained by these fits are identical to those determined by the simplified expressions, i.e., -1.06×10^4 and -6.23×10^3 erg/cm^3 for Fe films on GaN(0001) and GaN(000$\bar{1}$), respectively. Using these values and that of 2.2×10^4 erg/cm^3 for K_2 determined in [6], we obtain almost-identical values for K_3 for Fe films on GaN(0001) and GaN(000$\bar{1}$), namely, 9.19×10^5 and 9.21×10^5 erg/cm^3, respectively.

K_3 as determined from these experiments is unexpectedly large, namely, almost 50 times larger than K_2 and twice as large as K_1. This result gives rise to the question whether these values could be an artifact produced by the unequal area fraction of the multiple domains mentioned above. However, we have used the full expressions for the magnetocrystalline energy, and the term proportional to K_1 was thus fully taken into account. The impact of an unequal area fraction on the in-plane RMC is shown in Figs. 4(a)–4(c). Evidently, even a slight deviation from an equal partitioning results in a pronounced change in the curves. Moreover, Figs. 4(d)–4(g) show that for significantly smaller values of K_3, the RMC would be essentially isotropic. To obtain the sixfold symmetry and to reproduce the amplitude of the modulation observed in the experiment, K_3 needs to be of the same magnitude as obtained from the fits in Fig. 3.

To critically examine these data, we investigate the samples by an independent technique: FMR spectroscopy. We measured the magnetic anisotropy of the samples by FMR at a frequency ω_0 of 9.0 GHz. An external field was applied in-plane in different directions at room temperature. For Fe films on GaN(0001), the azimuthal angle dependence of the FMR spectra and resonance field H_r are shown in Fig. 5(a). The resonance fields with the magnetic field parallel ($H_r^{\parallel}$) and perpendicular ($H_r^{\perp}$) to the easy axis are 400 and 705

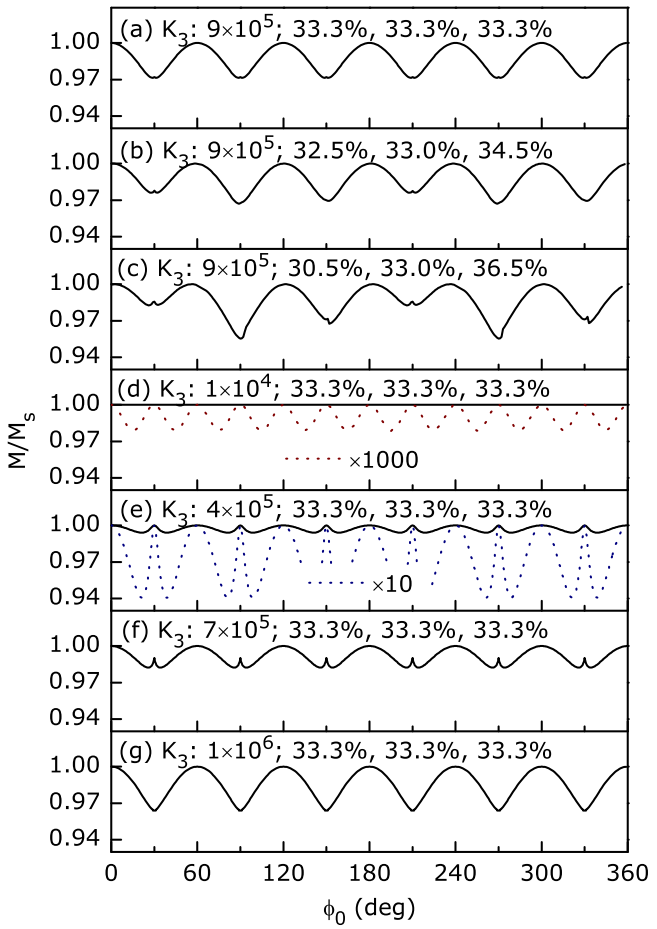

FIG. 4. (Color online) Calculated in-plane RMCs of Fe films on GaN(0001) with $K_1 = 4.7 \times 10^5$ and $K_2 = 2.2 \times 10^4$ erg/cm^3. (a–c) K_3 was assumed to have a value of 9×10^5 erg/cm^3, and the area fractions were changed as indicated. (d–g) We have kept the area fraction constant and, instead, varied K_3. For all curves, the magnetic field of 200 Oe was assumed to be parallel to the surfaces.

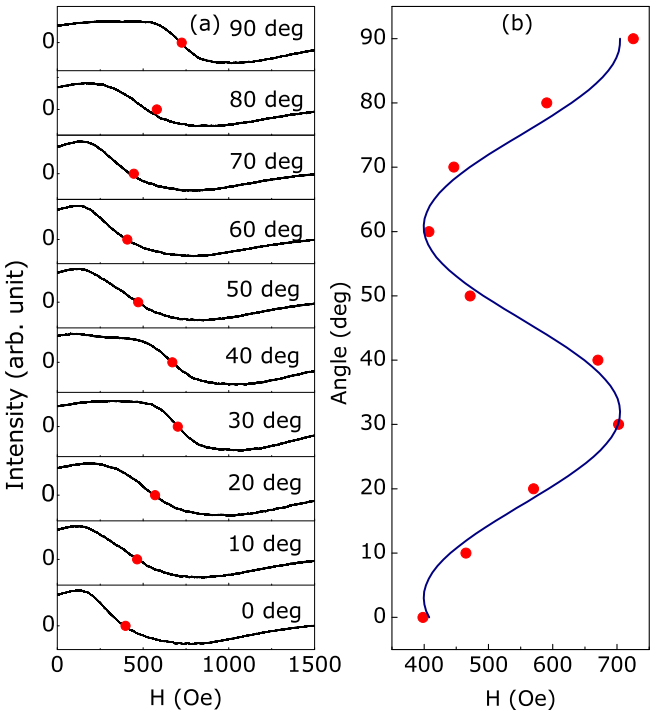

FIG. 5. (Color online) (a) In-plane angular dependence of the first derivative of FMR spectra obtained at room temperature with the magnetic field parallel to the surface for the Fe film on GaN(0001). (b) Experimental resonance field $H_r(\phi_0)$ [filled (red) circles] and the fit by a sine [solid (blue) line].

Oe, respectively, as shown in Fig. 5(b). Theoretically, the resonance frequency ω_0 for a planar system is given by $(\omega_0/\gamma)^2 = BH$ with the gyromagnetic ratio γ [22]. Here, we assume that γ and the value of B are independent of the in-plane azimuthal angle ϕ, which implies that the value of the static field H is independent of ϕ as well. Within the concept of the anisotropy energy in terms of an equivalent magnetic field [22], the in-plane anisotropy field is defined by $H_A = M_s^{-1}\partial^2\epsilon_A^{0001}/\partial\phi^2$ [23,24]. Combining this result with Eq. (3), we obtain $H_A = -36A_3M_s^{-1}\cos 6\phi$. Setting $\phi = 0^\circ$ for $H_A^{\parallel}$ and $\phi = 90^\circ$ for $H_A^{\perp}$, we obtain $36A_3/M_s = (H_r^{\parallel} - H_r^{\perp})/2$ with $H = H_A^{\parallel} + H_r^{\parallel} = H_A^{\perp} + H_r^{\perp}$. From the fit depicted in Fig. 5(b), $A_3 = -5.7 \times 10^3$ erg/cm^3.

In the same way, Figs. 6(a) and 6(b) show the FMR spectra of Fe films on GaN(000$\bar{1}$) and the resonance fields as a function of the azimuthal angle ϕ, respectively. From the fit to the latter, we obtain $H_r^{\parallel} = 470$ Oe and $H_r^{\perp} = 690$ Oe, and thus $A_3 = -4.2 \times 10^3$ erg/cm^3.

Using these values for A_3 and $K_2 = 2.2 \times 10^4$ erg/cm^3 [6], we obtain a K_3 of 4.70×10^5 erg/cm^3 for Fe films on

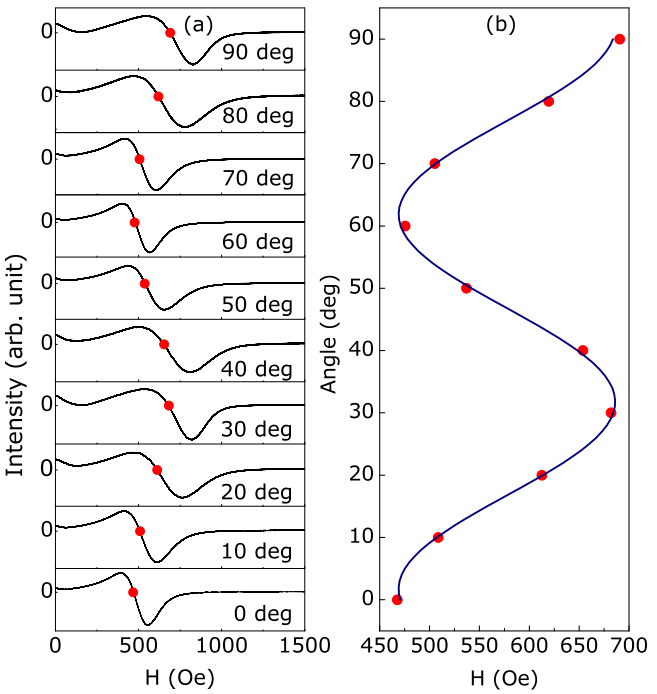

FIG. 6. (Color online) (a) In-plane angular dependence of the first derivative of FMR spectra obtained at room temperature with the magnetic field parallel to the surface for the Fe film on GaN(000$\bar{1}$). (b) Experimental resonance field $H_r(\phi_0)$ [filled (red) circles] and the fit by a sine [solid (blue) line].

GaN(0001) and 6.15×10^5 erg/cm^3 by for Fe films on GaN(000$\bar{1}$). These values are slightly smaller than those obtained by RMC. This deviation is no surprise since RMC is quasistatic, while FMR is a dynamic technique for which our analysis holds only approximately. Most important, however, is the fact that the values obtained by FMR are of the same order of magnitude as those determined by RMC. The fact that two entirely dissimilar experimental techniques arrive at essentially the same result confirms that the anisotropy constant K_3 for Fe is indeed unexpectedly large, namely, at least as large as K_1. For future studies of the magnetic anisotropy of Fe films, the term proportional to K_3 therefore cannot, in general, be neglected. Besides this insight, it would be most desirable to understand the physical reason for the unexpectedly large values of K_3 for Fe. To attain this understanding, we need to identify the mechanisms determining the magnitude of the higher-order anisotropy constants of the metallic ferromagnets Fe, Ni, and Co.

We thank Steven Erwin for helpful discussions and a critical reading of the manuscript. Our work was supported by the National Basic Research Program of China (Grant No. 2012CB933101), the National Natural Science Foundation of China (Grant Nos. 11274147 and 51371093), PCSIRT (Grant No. IRT1251), and Fundamental Research Funds for the Central Universities (Grant No. lzujbky-2013-ct01).

[1] J. H. Van Vleck, Phys. Rev. **52**, 1178 (1937).
[2] D. S. Wang, R. Q. Wu, and A. J. Freeman, Phys. Rev. Lett. **70**, 869 (1993).
[3] S. V. Halilov, A. Y. Perlov, P. M. Oppeneer, A. N. Yaresko, and V. N. Antonov, Phys. Rev. B **57**, 9557 (1998).
[4] Y. N. Zhang, J. X. Cao, I. Barsukov, J. Lindner, B. Krumme, H. Wende, and R. Q. Wu, Phys. Rev. B **81**, 144418 (2010).
[5] C. H. Du, R. Adur, H. L. Wang, A. J. Hauser, F. Y. Yang, and P. C. Hammel, Phys. Rev. Lett. **110**, 147204 (2013).
[6] H. L. Liu, W. He, H. F. Du, Y. P. Fang, Q. Wu, X. Q. Zhang, H. T. Yang, and Z. H. Cheng, Chin. Phys. B **21**, 077503 (2012).
[7] J. Ye, W. He, Q. Wu, H. L. Liu, X. Q. Zhang, Z. Y. Chen, and Z. H. Cheng, Sci. Rep. **3**, 2148 (2013).
[8] Y. T. Wang, F. Z. Lv, O. Brandt, J. Herfort, C. X. Gao, and D. S. Xue, Ann. Phys. **526**, L1 (2014).
[9] S. Chikazumi, *Physics of Ferromagnetism*, 2nd ed. (Oxford University Press, New York, 1997), pp. 250–254.
[10] C. D. Graham Jr., Phys. Rev. **112**, 1117 (1958).
[11] H. Gengnagel and U. Hofmann, Phys. Stat. Sol. **29**, 91 (1968).
[12] E. P. Wohlfarth, *Ferromagnetic Materials*, Vol. 1 (North-Holland, Amsterdam, 1980), pp. 38–39.
[13] B. D. Cullity and C. D. Graham, *Introduction to Magnetic Materials*, 2nd ed. (John Wiley & Sons, Hoboken, NJ, 2009), p. 201.
[14] M. Kak, R. Stephan, A. Mehdaoui, D. Berling, D. Bolmont, G. Gewinner, and P. Wetzel, Surf. Sci. **566–568**, 278 (2004).
[15] G. Garreau, S. Hajjar, J. L. Bubendorff, C. Pirri, D. Berling, A. Mehdaoui, R. Stephan, P. Wetzel, S. Zabrocki, G. Gewinner, S. Boukari, and E. Beaurepaire, Phys. Rev. B **71**, 094430 (2005).
[16] C. X. Gao, O. Brandt, S. C. Erwin, J. Lähnemann, U. Jahn, B. Jenichen, and H.-P. Schönherr, Phys. Rev. B **82**, 125415 (2010).
[17] C. X. Gao, O. Brandt, H.-P. Schönherr, U. Jahn, J. Herfort, and B. Jenichen, Appl. Phys. Lett. **95**, 111906 (2009).
[18] C. X. Gao, H.-P. Schönherr, and O. Brandt, Appl. Phys. Lett. **97**, 031906 (2010).
[19] C. X. Gao, O. Brandt, J. Lähnemann, J. Herfort, H.-P. Schönherr, U. Jahn, and B. Jenichen, J. Cryst. Growth **323**, 359 (2011).
[20] D. S. Xue, X. L. Fan, and C. J. Jiang, Appl. Phys. Lett. **89**, 011910 (2006).
[21] X. L. Fan, D. S. Xue, C. J. Jiang, Y. Gong, and J. Y. Li, J. Appl. Phys. **102**, 123901 (2007).
[22] C. Kittel, Phys. Rev. **73**, 155 (1948).
[23] H. B. G. Casimir, J. Smit, U. Enz, J. F. Fast, H. P. J. Wijn, E. W. Gorter, A. J. W. Duyvesteyn, J. D. Fast, and J. J. de Jong, J. Phys. Radium **20**, 360 (1959).
[24] O. Yalcin, *Ferromagnetic Resonance—Theory and Applications* (InTech, Rijeka, Croatia, 2013), pp. 12–15.